Making metals transparent: a circuit model approach

Carlos Molero,[1] Francisco Medina,[2,*] Raúl Rodríguez-Berral,[1] and Francisco Mesa[1]

[1]*Departamento Física Aplicada 1, ETS Ingeniería Informática, Universidad de Sevilla, Seville, 41012, Spain*

[2]*Departamento Electrónica & Electromagnetismo, Facultad de Física, Universidad de Sevilla, Seville, 41012, Spain*

[*]*medina@us.es*

Abstract: Solid metal films are well known to be opaque to electromagnetic waves over a wide frequency range, from low frequency to optics. High values of the conductivity at relatively low frequencies or negative values of the permittivity at the optical regime provide the macroscopic explanation for such opacity. In the microwave range, even extremely thin metal layers (much smaller than the skin depth at the operation frequency) reflect most of the impinging electromagnetic energy, thus precluding significant transmission. However, a drastic resonant narrow-band enhancement of the transparency has recently been reported. The quasi-transparent window is opened by placing the metal film between two symmetrically arranged and closely spaced copper strip gratings. This letter proposes an analytical circuit model that yields a simple explanation to this unexpected phenomenon. The proposed approach avoids the use of lengthy numerical calculations and suggests how the transmissivity can be controlled and enhanced by manipulating the values of the electrical parameters of the associated circuit model.

OCIS codes: (050.1950) Diffraction gratings; (260.3910) Metal optics; (240.0310) Thin films.

References and links

1. T. W. Ebbesen, H. J. Lezec, H. F. Ghaemi, T. Thio and P. A. Wolff, "Extraordinary optical transmission through sub-wavelength hole arrays," Nature (London) **391**, 667–669 (1998).
2. J. B. Pendry, L. Martín-Moreno and F. J. García-Vidal, "Mimicking surface plasmons with structured surfaces," Science **305**(5685), 847–848 (2004).
3. F. J. García-de-Abajo, "Colloquium: light scattering by particle and hole arrays," Rev. Mod. Phys. **79**(4), 1267–1290 (2007).
4. F. J. García-Vidal, L. Martín-Moreno, T. W. Ebbesen and L. Kuipers,"Light passing through subwavelength apertures," Rev. Mod. Phys. **82**(1), 729–787 (2010).
5. F. Medina, F. Mesa and R. Marqués, "Extraordinary transmission through arrays of electrically small holes from a circuit theory perspective," IEEE Trans. Microw. Theory Technol. **56**(12), 3108–3120 (2008).
6. F. Medina, F. Mesa and D. C. Skigin, "Extraordinary transmission through arrays of slits: a circuit theory model," IEEE Trans. Microw. Theory Technol. **58**(1), 105–115 (2010).
7. A. Alu, G. D'Aguanno, N. Mattiucci and M. J. Bloemer, "Plasmonic Brewster angle: broadband extraordinary transmission through optical gratings," Phys. Rev. Lett. **106**(12), 123902 (2011).
8. I. R. Hooper, T. W. Preist and J. R. Sambles, "Making tunnel barriers (including metals) transparent," Phys. Rev. Lett. **97**(5), 053902 (2006).
9. R. Dragila, B. Luther-Davies and S. Vukovic, "High transparency of classically opaque metallic films," Phys. Rev. Lett. **55**(10), 1117–1120 (1985).
10. L. Zhou, W. Wen, C. T. Chan and P. Sheng, "Electromagnetic-wave tunneling through negative-permittivity media with high magnetic fields," Phys. Rev. Lett. **94**(24), 243905 (2005).

#259951 Received 23 Feb 2016; revised 23 Apr 2016; accepted 25 Apr 2016; published 2 May 2016

11. Z. Song, Q. He, S. Xiao and L. Zhou, "Making a continuous metal film transparent via scattering cancellations," Appl. Phys. Lett. **101**(18), 181110 (2012).
12. J. D. Edmunds, M. J. Lockyear, A. P. Hibbins, J. R. Sambles and I. J. Youngs, "Resonantly overcoming metal opacity," Appl. Phys. Lett. **102**(1), 011120 (2013).
13. R. Rodríguez-Berral, C. Molero, F. Medina and F. Mesa, "Analytical wideband model for strip/slit gratings loaded with dielectric slabs," IEEE Trans. Microw. Theory Technol. **60**(12), 3908–3918 (2012).
14. D. M. Pozar, *Microwave engineering* (John Wiley & Sons Inc, 2005).
15. CST Microwave Studio, `https://www.cst.com/products/CSTMWS/`, accessed Dec. 2015.

1. Introduction

Triggered by the discovery of the extraordinary optical transmission (EOT) [1], a lot of research has been conducted to elucidate the nature of the enhanced frequency-selective transmission of electromagnetic waves through opaque (mostly metallic) screens periodically perforated with arrays of sub-wavelength holes or slits. Nowadays this phenomenon is known to occur at any frequency from microwaves to optics and it is well understood in terms of the excitation of (spoof) surface plasmon-polaritons [2–4]. Alternative models [5,6] based on impedance matching conditions are also available. Enhanced transmission is usually observed in a rather narrow frequency band, although ultra-wideband transparency can be obtained for specific angles of incidence through structured metal slabs involving sub-wavelength apertures [7]. However, the transmission of electromagnetic waves through solid metal films (i.e., continuous, non-structured) is always very weak, even though thin metal screens are involved. At optical frequencies, the reason for such high opacity is related to the high and negative real part of the metal permittivity (lossy plasma behavior), which results in a purely imaginary refractive index. In such circumstances the transverse electromagnetic waves inside metals become evanescent; namely, exponentially decaying in amplitude. In [8] it has been reported that, to some extent, a thin metal layer illuminated with an optical-frequency plane wave behaves as an analogous to a tunnel barrier. Thus, several techniques have been proposed in the literature to achieve a significant increase of the optical transmissivity in a given frequency band [8–11]. Although the experimental results reported in [10, 11] were obtained at microwave frequencies, the opaque layers employed in those works were actually "effective surfaces" that mimic the behavior of solid metal films at the optical range (i.e., they were not true solid metal films but rather properly designed metasurfaces).

From THz down to microwaves or even DC, the electrical response of metals is well described in terms of a large real conductivity. If the thickness of the metal layer is meaningfully larger than the skin depth at the working frequency (at least two or three times larger), attenuation is too strong as to allow for relevant transmissivity through the solid metal slab. Moreover, even extremely thin metal films, having a thickness of a few tens of nanometers (i.e., well below the typical skin depth for metals at microwave frequencies), are also very opaque. Since absorption is marginal in this case, opacity here comes from the strong reflection caused by the abrupt impedance mismatching associated with the presence of the thin metallic film. Nevertheless, the possibility of opening a narrow transmission window in the microwave region has recently been reported in [12] by introducing an auxiliary periodically structured surface. More specifically, the authors of [12] show the appearance of a strong narrow-band transmission peak around 22.7 GHz using an electrically ultra-thin resonant structure attached to a 60 nm thick solid aluminum film (the aluminum film alone, in spite of its small thickness, would not allow for a significant transmission of microwave power through it). The thin aluminum film was placed between a couple of identical copper strip gratings separated from the film by an electrically thin dielectric layer of approximately $5\times10^{-4}\lambda_0$ thickness, with λ_0 being the wavelength in vacuum at 22.7 GHz. The basic operational structure is represented in Fig. 1. In the experimental setup used in [12] a number of additional external dielectric layers were used, and

#259951 Received 23 Feb 2016; revised 23 Apr 2016; accepted 25 Apr 2016; published 2 May 2016

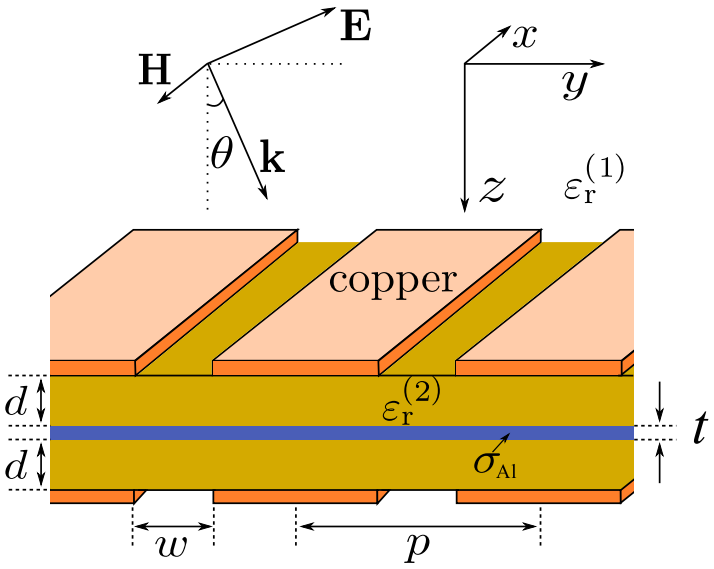

Fig. 1. Sketch of a basic structure exhibiting enhanced frequency-selective transmission through a thin solid metal (aluminum) film of extremely small thickness ($t = 60\,\text{nm}$). TM incidence is assumed. A similar structure, including some additional external layers required by the experimental setup, was shown to exhibit enhanced transmission around a certain frequency in the microwave range in [12].

a small air gap was supposed to exist within the sandwiched structure.

The purpose of the present letter is to give a physically insightful explanation of the experimental results reported in [12] at the light of the accurate equivalent circuit (EC) modeling technique previously developed by the authors in [13]. In that work it was discussed the modeling of the reflection and transmission properties of a variety of strip–like and slit–like metal gratings embedded in (or printed on) layered dielectric media. The EC models in [13], systematically derived using an *ab initio* approach, give a convenient analytical solution to the problem and, at the same time, yield a simple conceptual frame that make it easier the design of devices based on those structures. In the present letter, the approach in [13] is supplemented in order to include the presence of the solid metal film. Although the modifications introduced in the model are relatively simple (but not trivial), they provide the fundamental physics that explains the existence of resonant transmission. Thus, the reported analytical methodology does not only avoid the use of lengthy and demanding computational tools but, more importantly, renders an insightful alternative point of view that reveals the relevant structural parameters to be adjusted in order to control the transmissivity. The details of the derivation of the circuit model and the involved approximations are given in Sec. 2. In Sec. 3 the results obtained with the proposed model are shown to explain the experimental observation in [12]. It is also shown how the structure can be modified in order to enhance the transmissivity level and to tune the resonance frequency.

2. Derivation of the analytical circuit model

In the structure shown in Fig. 1, an extremely thin metal film is sandwiched between two electrically thin dielectric layers where two identical strip gratings of copper have been etched. The structure is illuminated with a TM-polarized plane wave (magnetic field parallel to the slits of the gratings). Due to the periodic nature of the problem, only the single unit cell shown in

#259951 Received 23 Feb 2016; revised 23 Apr 2016; accepted 25 Apr 2016; published 2 May 2016

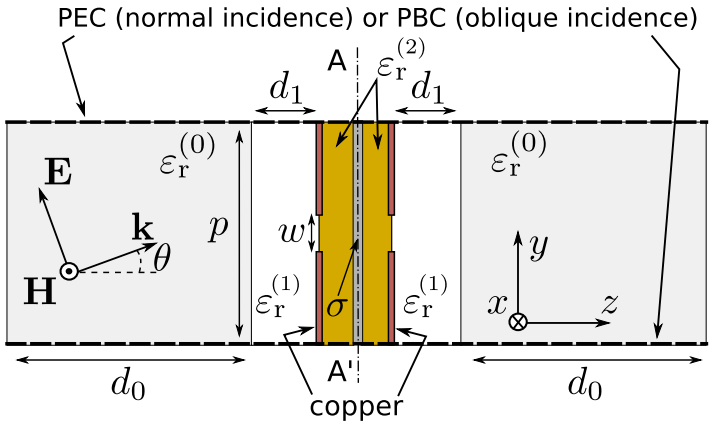

Fig. 2. Basic unit cell for the analysis of the structure in [12]. TM incidence is assumed. PEC stands for perfect electric conductor and PBC for periodic boundary conditions.

Fig. 2 has to be considered for analysis purposes. In that unit cell, some additional external dielectric layers have been incorporated in order to account for the actual experimental setup used in [12]. Note that the size of this unit cell along the x-axis can be arbitrarily chosen since there is no variation of the electromagnetic quantities along the x direction. In our case, this size has been taken equal to the period of the structure along the y-direction, p. For normal incidence, the horizontal boundaries (perpendicular to the impinging electric field) of the unit cell behave as virtual perfect electric conductors (PEC) whereas the vertical walls (perpendicular to the impinging magnetic field) would behave as perfect magnetic conductors (PMC). Oblique TM incidence can be incorporated in a trivial manner by substituting the PEC walls by periodic boundary conditions (PBC). In the experiment carried out in [12], the structural and electrical parameters were: $p = 3.80\,\text{mm}$, $w = 0.120\,\text{mm}$, $d_0 = 7.44\,\text{mm}$, $d_1 = 0.80\,\text{mm}$, $d = 75\,\mu\text{m}$, $t = 60\,\text{nm}$, $\varepsilon^{(0)} = \varepsilon_0(2.6 + \text{i}0.15)$, $\varepsilon^{(1)} = \varepsilon_0(4.1 + \text{i}0.082)$ (commercial FR4 PCB substrate), $\varepsilon^{(2)} = 2.6\varepsilon_0$, $\sigma_{\text{Al}} = 1.12 \times 10^7\,\text{S/m}$. The value of the conductivity has been chosen to be consistent with the equivalent permittivity used in the numerical simulations in [12] (it is not the bulk conductivity of aluminum but some effective value accounting for surface effects associated with the small value of the thickness t). The thickness of the aluminum film, despite being so small, is enough to almost totally shield microwave radiation in the absence of the copper grating.

The analysis of structures with this geometry, excluding the thin metal film, was carried out by the authors in [13] by means of an analytical formulation that led to an equivalent circuit (EC). Following the guidelines in [13], it is clear that the unit cell in Fig. 2 can be viewed as a parallel-plate transmission line system whose boundaries are two parallel PEC walls (normal incidence case) separated a distance equal to the period of the grating, p, and two arbitrarily separated magnetic walls perpendicular to the PEC boundaries. As a separation of p is taken here, the characteristic admittance of the parallel-plate waveguides in each of the dielectric regions is simply given by $Y_0^{(j)} = \sqrt{\varepsilon_r^{(j)}}\sqrt{\varepsilon_0/\mu_0}$ $(j = 0, 1, 2)$. The resulting guiding system in Fig. 2 presents a number of discontinuities along the z-direction. The dielectric-to-dielectric interfaces do not generate new modes whereas an infinite number of high-order TM modes are scattered by the metalized discontinuities (copper gratings). The propagating electromagnetic waves in each of the regions can be represented by simple transmission line sections [14] whereas the effect of the localized (evanescent) high-order TM modes scattered by the slits can be accounted for by means of lumped capacitors. This modeling is possible provided the oper-

#259951 Received 23 Feb 2016; revised 23 Apr 2016; accepted 25 Apr 2016; published 2 May 2016

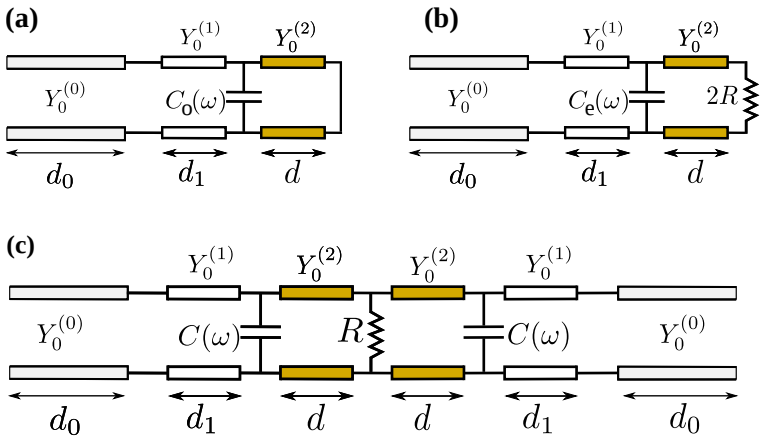

Fig. 3. (a) EC for odd excitation of the unit cell in Fig. 2 (a virtual electric wall in the central middle plane, AA', is modeled through a short-circuit termination); (b) EC for even excitation (a low resistance of value $2R$ substitutes the short-circuit used for the odd-excitation case; (c) EC representing the unit cell in Fig. 2 when $C_e = C_o$.

ation frequency is low enough to preclude the excitation of propagating high-order TM modes in the dielectric regions around the slits [13], as happens in the experiment carried out in [12].

The ECs shown in Figs. 3(a) and 3(b) are suitable representations of the electromagnetic problem sketched in Fig. 2 assuming symmetrical (even) and anti-symmetrical (odd) excitations. The reflection coefficients for the impinging voltage waves in these circuits will allow us to compute the reflection (S_{11}) and transmission (S_{21}) coefficients for the fundamental propagating mode that impinges on the periodic layered structure in Fig. 2. Note that the superposition principle can be invoked [14] to express S_{ij} in terms of the reflection coefficients, S_{11}^{o} and S_{11}^{e}, for the two circuits in Figs. 3(a) and 3(b); i.e., $S_{11} = (S_{11}^{o} + S_{11}^{e})/2$ and $S_{21} = (S_{11}^{e} - S_{11}^{o})/2$ (the superscript "o" stands for odd excitation and "e" for even excitation). It should be taken into account that for odd/even- excitation the vertical symmetry plane in Fig. 2 (AA') is a virtual short/open circuit. Thus, the EC for odd-excitation operation is the one depicted in Fig. 3(a) and the EC accounting for even-excitation operation is shown in Fig. 3(b). The aluminum film is represented by means of a simple resistor, $2R = 2/(\sigma_{Al} t)$ ($R \approx 1.49\,\Omega$ if the value of the effective σ_{Al} in [12] is taken). The DC formula for the resistance can be used here because $t \ll \delta$ in the frequency range of interest (δ is the skin depth in the aluminum layer). Note that the effect of the ultra-thin aluminum layer only appears in the EC for even-excitation operation in Fig. 3(b) since the virtual short-circuit in Fig. 3(a) at the end of the transmission line section accounting for the $75\,\mu$m dielectric layer is connected in parallel with the resistor.

The capacitances $C_o(\omega)$ and $C_e(\omega)$ in Figs. 3(a) and 3(b) account for the presence of the copper grating. The dependence on frequency comes from the contribution of the first excited high-order TM mode, whose cutoff frequency is not high enough as to make this contribution frequency-independent [13]. In principle, $C_o(\omega)$ and $C_e(\omega)$ are expected to be different due to the strong coupling between the closely spaced gratings through high-order modes generated at the slit discontinuity [13]. Indeed, the difference between those capacitances would be very important if the aluminum film was not present. Fortunately, the low resistivity of the metal film drastically simplifies the situation. For odd-excitation, as mentioned above, the equivalent resistor is virtually short-circuited and the value of $C_o(\omega)$ would be the one obtained for a single grating backed by a PEC ground plane placed at a distance d from the grating. This value can easily be computed using the analytical expressions provided in [13] for such geometry. For

#259951 Received 23 Feb 2016; revised 23 Apr 2016; accepted 25 Apr 2016; published 2 May 2016

even-excitation it is key to note that the resistor loading the even excitation equivalent circuit ($2R$) has a very low value in comparison with the characteristic impedances of the transmission lines involved in the circuit model. It makes the even-excitation physical situation be almost indistinguishable from the odd-excitation one, and hence C_e will be approximately equal to C_o. The presence of the lossy aluminum film would also make C_e be complex; i.e., it would incorporate a frequency-dependent conductance. However, the imaginary part of C_e coming from the presence of the aluminum film would also be negligible and, therefore, we can consider $C_e = C_o = C(\omega)$ and real (a minimal error below 0.3% is estimated). This is an interesting result since, under this approximation, the equivalent circuit in Fig. 3(c) can be used to model the whole structure, thus avoiding the necessity of considering separated even- and odd-excitation circuits. Note that the resistor R, which only affects the fundamental mode [the effect of all high-order modes is embedded in $C(\omega)$] will account for the absorption in the metal film and the mismatching return losses. The small real part of the admittance associated with high-order modes embedded in C_e can be completely neglected.

In order to understand the appearance of the strong transmission peak reported in [12], first it should be considered that, in the absence of the thin metal film as well as dielectric losses, perfect transmission would be allowed at those frequencies for which $S_{11}^e = -S_{11}^o$ [13]. Using the equivalent circuits in Figs. 3(a) and 3(b), it is straightforward to understand that the phase difference between S_{11}^e and S_{11}^o can reach a value of π radians at some frequency point very close to the resonance of the resonator formed by $C_o(\omega)$ and the short-circuited transmission line section appearing in Fig. 3(a), since the even-excitation equivalent circuit does not resonate in this range of frequencies. As that transmission line section is electrically short and loaded with a short-circuit, it could be substituted by a series frequency-independent inductor, $L = \mu_0 d$, if desired. Now, if we consider again that the aluminum film is present, it is found that the situation for even excitation is quite similar to the previous one, except for the existence of a low resistance load ($2R$) instead of a short circuit. This makes that S_{11}^e and S_{11}^o have almost the same amplitude and phase (thus yielding a very low value of S_{21}) except around the resonance frequency $\omega_{res} = 1/\sqrt{LC}$. Thus, within a narrow frequency band around this resonance frequency, S_{21} can reach relatively high values (much higher than in the absence of the copper gratings). This circumstance easily explains the existence of the strong transmissivity in [12] despite the presence of the, otherwise almost totally opaque, solid aluminum film. Examples of this phenomenon are reported in the following section.

3. Comparison with experimental results and discussion

A simple computer code has been implemented to calculate the values of the capacitances in the circuit shown in Fig. 3(c) from the dimensional and electrical parameters of the structure. More specifically, the capacitance used in our simulations has been obtained using the formulas given in [13] for the case of a metal grating printed on a stratified substrate with a PEC ground plane located at the position of the symmetry plane AA' (see Fig. 2). It is worth mentioning that this capacitance includes a frequency-dependent contribution associated with the first scattered TM mode since its variation with frequency is found of practical relevance. The values of the characteristic admittances of all the transmission line sections are known in closed form, as well as the propagation constants of the supported TEM waves. With these data, the calculation of S_{11}^e and S_{11}^o (and S_{11} and S_{12} for the circuit in Fig. 3(c)), is a trivial exercise [14]. The results obtained with this code have been validated by comparison with the data reported in [12], as plotted in Fig. 4. The blue solid line corresponds to our analytical EC results for the transmissivity ($|S_{12}|^2$) considering the structure shown in Fig. 2. If the air gaps empirically proposed in [12] are included in the model (it simply requires the addition of a short air-filled transmission line section to the model), the red line is obtained, which shows a better matching with the exper-

#259951 Received 23 Feb 2016; revised 23 Apr 2016; accepted 25 Apr 2016; published 2 May 2016

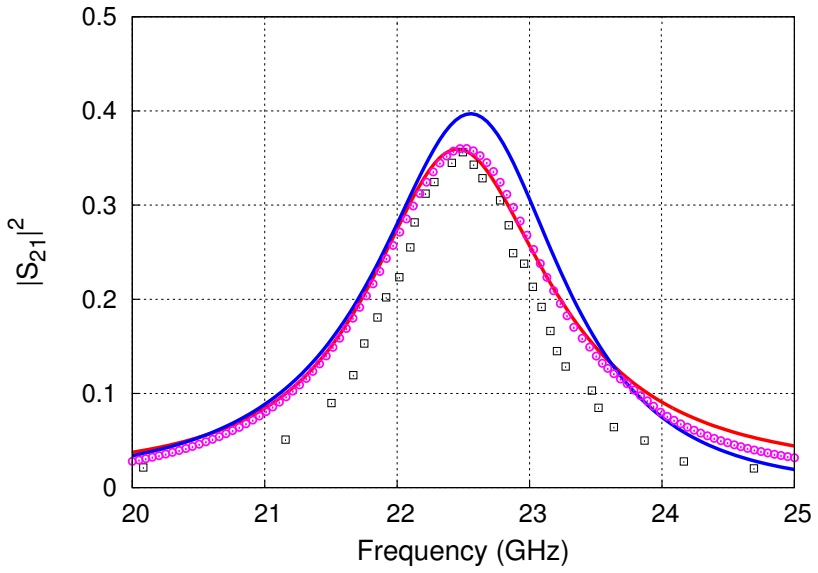

Fig. 4. Transmissivity of the structure experimentally studied in [12]. Squares are experimental data in that paper. The solid lines have been obtained with our circuit model (the red one includes the effect of a $10\,\mu$m air gap considered in [12]). Circles have been computed using *CST Microwave Studio* for the structure with the air gap. The electrical and dimensional parameters are given in the main text.

imental data. It can also be observed that the resonance frequency and the transmission level are very accurately reproduced by the proposed simple analytical model. Nevertheless, the predicted quality factor is slightly lower, although the authors have obtained a similar discrepancy in the quality factor when using the commercial electromagnetic simulator CST Microwave Studio [15], as it can be seen in Fig. 4. (It must be taken into account that the thickness of the air gap was empirically adjusted to accurately match the experimental resonance frequency; i.e. it was not actually measured). It is worth mentioning that, if the aluminum film is removed, the structure becomes almost totally transparent at the same resonance frequency. This fact is also well accounted for by our circuit model after using the appropriate values of C_o and C_e in the ECs in Figs. 3(a) and 3(b) (these values are different if the metal film is not present) and $R=\infty$.

In Fig. 5 we have plotted the magnitude and phase difference of the even- and odd- reflection coefficients. Dielectric losses have been neglected, in such a way that $|S_{11}^\mathrm{o}|=1$. It can be clearly observed that the maximum transmission frequency point corresponds to a phase difference of 180^o between the even and odd reflection coefficients. Most of the dependence with the frequency of the phase difference comes from the resonant behavior of the odd-excitation equivalent circuit, since the phase of S_{11}^e varies smoothly in this frequency range. At the resonance point, the magnitude of S_{11}^e is close to a minimum. It clearly suggests that this minimum should be as low as possible in order to increase the transmissivity. In any case, provided a phase difference of 180^o can be achieved, the minimum possible magnitude of the transmission coefficient is $|S_{21}|=0.5$. When this phase condition is satisfied, it is readily found that $|S_{21}|=(|S_{11}^\mathrm{e}|+|S_{11}^\mathrm{o}|)/2$. As $|S_{11}^\mathrm{o}|=1$ when dielectric losses are neglected, it is clear that $|S_{21}|\geq 0.5$. However, it should be mentioned that a 180^o phase difference between S_{11}^e and S_{11}^o cannot be achieved if the metal film resistance is too low, which happens below a threshold value of $R=0.57\,\Omega$ for the specific geometry under study. In such case, the transmissivity can actually be less than 0.5.

#259951 Received 23 Feb 2016; revised 23 Apr 2016; accepted 25 Apr 2016; published 2 May 2016

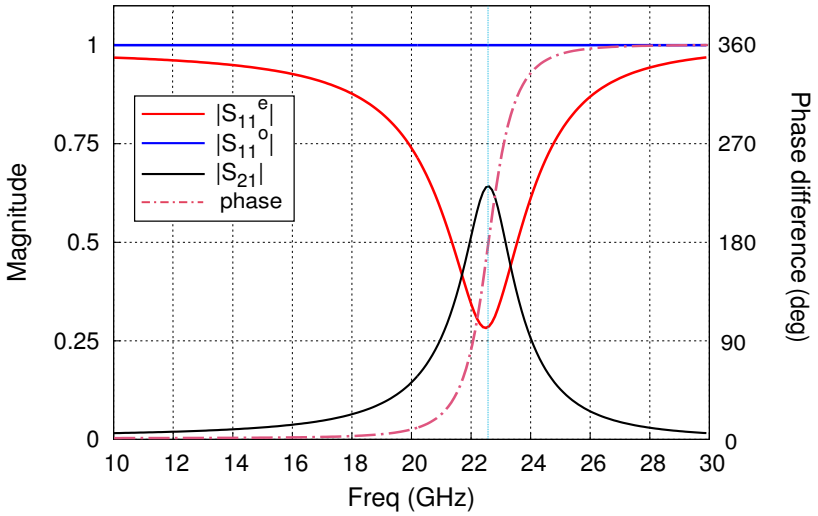

Fig. 5. Magnitude of S_{11}^{e} (solid red) and S_{11}^{o} (solid blue) and phase difference (dot-dashed line) between these two reflection coefficients as a function of frequency for the structure studied in [12]. The transmission coefficient $|S_{12}|$ has been also included (solid black). Dielectric losses have been ignored.

As already mentioned, the electrically short transmission line sections corresponding to the thin dielectric layers in contact with the aluminum film can be substituted by a simple inductor of value $L = \mu_0 d$. The resonance angular frequency for the odd-excitation circuit model is $\omega_{res}^{o} = 1/\sqrt{LC}$. At that frequency the impedance loading the odd-excitation circuit model would be an open circuit. The resonance angular frequency for the even-excitation circuit is slightly lower than ω_{res}^{o} due to the presence of the resistance $2R$. This resonance angular frequency is given by

$$\omega_{res}^{e} = \omega_{res}^{o}\left[1 - \left(\frac{2R}{\sqrt{L/C}}\right)^{2}\right] \approx \omega_{res}^{o} \tag{1}$$

where it has been taken into account that $R \ll \sqrt{L/C}$ for typical values of the involved electrical parameters. At the resonance frequency ω_{res}^{e}, the even-excitation circuit model is found to be loaded with a real impedance given by $R_{res}^{e} = L/(2RC)$. In order to enhance transmissivity at resonance, this loading impedance should be made much smaller than the characteristic impedances of the involved transmission line sections. Now, to keep the discussion as simple as possible, let us consider the simplified version of the problem in Fig. 1, where a single dielectric medium exists at both sides of the sandwiched structure. According to the above discussions, the transmissivity at resonance can be increased by making S_{11}^{e} as close to -1 as possible, since $S_{11}^{o} = +1$ at that resonance frequency and $S_{12} = (S_{11}^{e} - S_{11}^{o})/2$. It means that R_{res}^{e} has to be adjusted to be small in comparison with the transmission line characteristic impedance. For a given value of R (imposed by the metal film conductivity and thickness), this can be done by decreasing the value of L (i.e., reducing the thickness d of the internal dielectric layer) and/or by increasing the value of C. The capacitance C can be increased by reducing the value of w, but this might lead to fabrication problems. An alternative path to increase C is to use a meandered slit. Fig. 6 shows the consequences of introducing a meandered slit in a simple structure with all the dielectric materials assumed to be lossless and considering a single external dielectric medium (only a lossless medium with permittivity $\varepsilon^{(1)} = 4.1\varepsilon_0$ is assumed in the external region

#259951 Received 23 Feb 2016; revised 23 Apr 2016; accepted 25 Apr 2016; published 2 May 2016

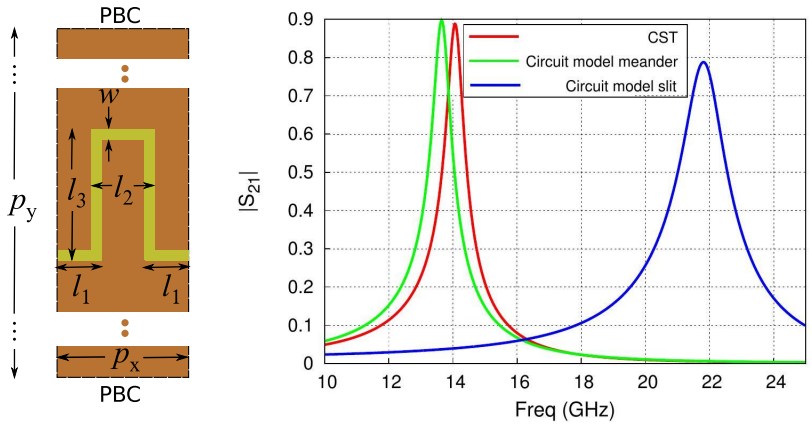

Fig. 6. Magnitude of the transmission coefficient through the structure in Fig. 2 (dielectric and copper losses are neglected) without the layer characterized by $\varepsilon^{(0)}$. The solid blue curve corresponds to a uniform straight slit. Green (analytical) and red (numerical, CST) curves correspond to the same structure with a meandered slit (total length = $2.76\,p$). The unit cell of the simulated meandered structure is depicted in the left panel (only the front view is shown since the dielectric configuration is the same used for the uniform slit). The top and bottom walls are periodic boundary conditions (PBC) whereas the left and right boundaries of the unit cell are magnetic walls. Dimensions: $p_x = 1.0\,\text{mm}$, $p_y = 3.8\,\text{mm}$, $w = 0.12\,\text{mm}$, $l_1 = 0.34\,\text{mm}$, $l_2 = 0.56\,\text{mm}$, $l_3 = 1.0\,\text{mm}$.

in Fig. 2). In this way, the only source of losses is the thin aluminum film. No air gap is considered in this case. The resonance of the structure with the straight slit is slightly below 22 GHz and the amplitude of the transmission coefficient at resonance is about 0.79. Meandering the slit in such a way that its length per unit cell (p.u.c.) is 2.76 times the width of the unit cell (p) gives a significantly higher p.u.c. capacitance. Simulations carried out with CST Microwave Studio [15] and with our circuit model using a rough estimated value of the meandered slit capacitance show that the resonance frequency is clearly reduced as well as the transmissivity is meaningfully increased (see Fig. 6). Our rough estimation of the meandered slit capacitance has been obtained by analytically solving for a straight slit and determining its per unit length (p.u.l.) capacitance; the total capacitance of the meandered slit is then considered to be approximately given by such p.u.l. capacitance times the total length of the slit. The accuracy of our results for the meandered slit could be improved using a better estimation of the capacitance of the meandered capacitor. Nevertheless, the chosen example suffices to point out the good physical insight provided by the proposed circuit model and the consequent accurate prediction of the behavior of the structure.

Finally it will be explored how to modify the circuit model in order to predict the behavior of the structure under study when the metal film thickness is not negligible in comparison with the skin depth. Now the distributed effects of the fields inside the metal film should not be ignored. The aluminum film should be modeled as a highly lossy transmission line section. In such case, the EC for odd excitation is not terminated with a short-circuit but with the input impedance of a $t/2$ section of such lossy line terminated with a short circuit. The resistor, $2R$, loading the EC for the even excitation should be replaced by the input impedance of the same lossy line section terminated with an open circuit. These input impedances are analytically known using standard transmission line theory [14] with the appropriate complex values of the characteristic admittance and propagation constant, which are related to the skin depth in the aluminum at the working frequency. Note that those two complex loads for odd and even excitations collapse

#259951 Received 23 Feb 2016; revised 23 Apr 2016; accepted 25 Apr 2016; published 2 May 2016

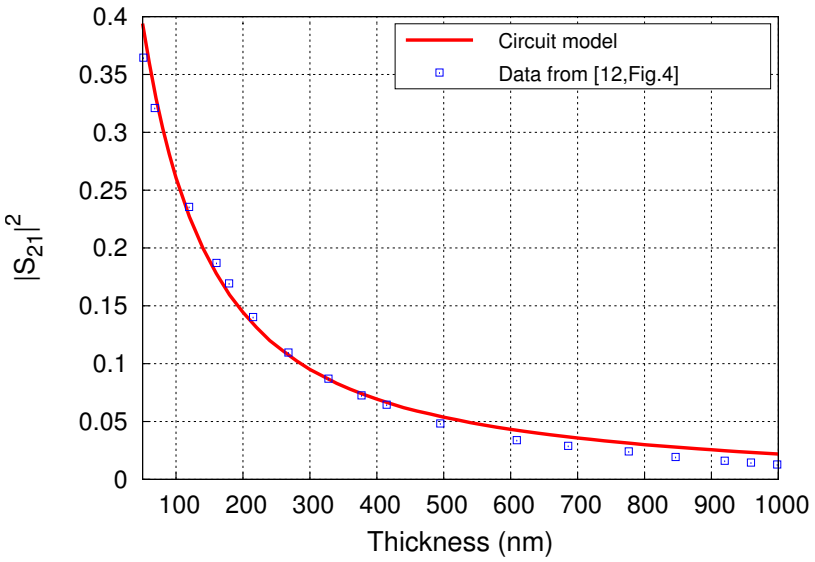

Fig. 7. Transmissivity as a function of the aluminum film thickness (analytical data versus numerical results in [12, Fig. 4].

into the same value for thick enough metal films (3 to 4 times the skin depth), in such a way that no transmission would be predicted by our model, as physically expected. For intermediate values of the film thickness, an exponential decay of the transmissivity is predicted by this analytical model. In Fig. 7 our analytical results are compared with the full-wave data provided in [12]. As a final comment, it is worth to say that, if the angle of incidence is different from zero (oblique incidence), the model is still valid using the angle dependence of the characteristic admittances of the transmission line sections, as explained in [13]. Our model is then able of reproducing the experimental angle dependence of the transmissivity reported in [12, Fig. 5].

4. Conclusion

A simple analytical circuit model has been developed to explain the observed enhanced frequency-selective transmission of electromagnetic waves through thin solid metal films at microwave frequencies when the film is sandwiched between two copper strip gratings. The model correctly predicts the experimentally observed and numerically computed transmission peak and suggests the way of controlling the resonance frequency and the transmissivity.

Acknowledgment

The authors acknowledge financial support from Spanish Ministerio de Economía y Competitividad and European Union FEDER funds (project TEC2013-41913-P) and Spanish Junta de Andalucía (project P12-TIC-1435).

#259951 Received 23 Feb 2016; revised 23 Apr 2016; accepted 25 Apr 2016; published 2 May 2016